Arianna Marino,[1] Rossella Menghini,[1] Marta Fabrizi,[1] Viviana Casagrande,[1] Maria Mavilio,[1] Robert Stoehr,[1] Eleonora Candi,[2] Alessandro Mauriello,[3] Jose M. Moreno-Navarrete,[4] María Gómez-Serrano,[5] Belén Peral,[5] Gerry Melino,[2,6] Renato Lauro,[1] Jose M. Fernandez Real,[4] and Massimo Federici[1,7]

<div style="writing-mode: vertical">**OBESITY STUDIES**</div>

ITCH Deficiency Protects From Diet-Induced Obesity

Classically activated macrophages (M1) secrete proinflammatory cytokine and are predominant in obese adipose tissue. M2 macrophages, prevalent in lean adipose tissue, are induced by IL-13 and IL-4, mainly secreted by Th2 lymphocytes, and produce the anti-inflammatory cytokine IL-10. ITCH is a ubiquitously expressed E3 ubiquitin ligase involved in T-cell differentiation and in a wide range of inflammatory pathways. ITCH downregulation in lymphocytes causes aberrant Th2 differentiation. To investigate the role of Th2/M2 polarization in obesity-related inflammation and insulin resistance, we compared wild-type and *Itch*$^{-/-}$ mice in a context of diet-induced obesity (high-fat diet [HFD]). When subjected to HFD, *Itch*$^{-/-}$ mice did not show an increase in body weight or insulin resistance; calorimetric analysis suggested an accelerated metabolism. The molecular analysis of metabolically active tissue revealed increased levels of M2 markers and genes involved in fatty acid oxidation. Histological examination of livers from *Itch*$^{-/-}$ mice suggested that ITCH deficiency protects mice from obesity-related nonalcoholic fatty liver disease. We also found a negative correlation between ITCH and M2 marker expression in human adipose tissues. Taken together, our data indicate that ITCH E3 ubiquitin ligase deficiency protects from the metabolic disorder caused by obesity.

Obesity is associated with a chronic state of low-grade inflammation, which predisposes to insulin resistance, type 2 diabetes, hepatic steatosis, and atherosclerosis (1–4). Obesity is also characterized by a progressive immune cell infiltration into adipose tissue (5). Among the immune cells infiltrating obese adipose tissue, adipose tissue macrophages (ATMs) play an important role in maintaining a continuous inflammatory state (1). Classical activated macrophages (M1) are induced by γ-interferon (IFN-γ); produce proinflammatory cytokines such as interleukin (IL)-1β, IL-6, and tumor necrosis factor (TNF)-α; and are predominant in obese adipose tissue (6,7). M2 macrophages are induced by Th2 lymphocyte–derived IL-13 and IL-4 cytokines and produce the anti-inflammatory cytokine IL-10. They are characterized by the expression of specific markers such as Arg1, Mgl2, YM1, and Mannose receptor are involved in tissue remodeling/repair and in fibrotic processes and are characteristic of adipose tissue from lean subject (8). IL-4, through STAT6 signaling, can induce the expressions of peroxisome proliferator–activated receptor (PPAR)-γ

---

[1]Department of Systems Medicine, University of Rome Tor Vergata, Rome, Italy
[2]Department of Experimental Medicine and Surgery, University of Rome Tor Vergata, Rome, Italy
[3]Department of Biopathology and Imaging, University of Rome Tor Vergata, Rome, Italy
[4]Department of Diabetes, Endocrinology and Nutrition, University Hospital of Girona "Dr. Josep Trueta," Institut d'Investigacio Biomedica de Girona IdibGi, and CIBER Fisiopatologia de la Obesidad y Nutricion, Girona, Spain
[5]Instituto de Investigaciones Biomédicas, Alberto Sols, Consejo Superior de Investigaciones Científicas and Universidad Autónoma de Madrid, and CIBER Fisiopatología de la Obesidad y Nutrición Istituto De Salud Carlos III, Madrid, Spain

[6]Toxicology Unit, Medical Research Council, Leicester, U.K.
[7]Center for Atherosclerosis, University Hospital "Policlinico Tor Vergata," Rome, Italy

Corresponding author: Massimo Federici, federicm@uniroma2.it.

Received 20 May 2013 and accepted 18 October 2013.

This article contains Supplementary Data online at http://diabetes .diabetesjournals.org/lookup/suppl/doi:10.2337/db13-0802/-/DC1.

and PPAR-γ coactivator (PGC)-1β and then contribute to fatty acid oxidation in M2 macrophages (9). ITCH is a ubiquitary E6-associated protein carboxyl terminus (Hect)-type E3 ubiquitin ligase originally identified studying the agouti locus whose mutation results in coat color alterations in mice (10). The *itch* gene encodes 854 amino acids with a relative molecular weight of 113 kDa. The non–agouti-lethal 18H or $Itch^{-/-}$ mice display severe immune and inflammatory defects. On the C57BL/6J background, *Itch* deficiency results in spontaneous development of a late-onset and progressively lethal systemic autoimmune-like diseases (11). $Itch^{-/-}$ T lymphocytes display increased production of Th2 cytokines (e.g., IL-4 and IL-5), causing biased differentiation of CD4$^+$ cells into Th2 cells and chronic activation (12). *Itch* disruption in α/β and γ/δ T cells causes expansion of B1b lymphocytes leading to IgM elevation and initiates IgE production, respectively (13). ITCH regulates the stability of both transmembrane receptors and intracellular substrates driving them to lysosomal and proteasomal degradation, respectively. Among ITCH substrates, there are modulators of the immune response, such as the Jun family members (c-Jun, JunB) and NOTCH as well as regulator of cell death, such as the p53 family members (p63, p73) (11). Here, we used the $Itch^{-/-}$ mice to clarify the roles of Th2/M2 polarization in obesity-related inflammation and in the progression of fatty liver disease.

RESEARCH DESIGN AND METHODS

Mouse Model and Metabolic Analysis

$Itch^{-/-}$ mice on a C57/BL10 background have previously been described (10–12). $Itch^{-/-}$ mice and wild-type (WT) littermates were maintained on 12-h light and dark cycles under controlled environmental conditions, with free access to water and food. Studies were performed only in male mice. Animal studies were approved by the University of Tor Vergata Animal Care and Use Committee. For the diet-induced obesity model, 6- to 8-week old mice were fed a high-fat diet (HFD) (60% of calories from fat; Research Diets, New Brunswick, NJ) or normal diet (ND) (standard chow 10% calories from fat; GLP Mucedola Srl, Settimo Milanese, Italy) for 12 weeks after weaning as indicated. Metabolic testing procedures have previously been described (14,15). Total cholesterol, HDL, triglycerides, aspartate aminotransferase (AST) and alanine aminotransferase (ALT) levels were measured using Keylab (BPC Biosed s.r.l., Rome Italy). The tissues were collected in the fasting or refed state as indicated. In the fasting experiments, animals were fasted for 16 h. In the refeeding experiments, food was reintroduced after 16 h of fasting and the animals were killed 6 h after refeeding to isolate the tissues. Indirect calorimetry was performed as previously described (16).

Isolation of Murine Peritoneal Macrophages

Peritoneal macrophages were isolated from WT and $Itch^{-/-}$ mice and characterized as previously described

(17). Briefly, macrophages were collected from mice that were previously injected with 1 mL of 3% thioglycollate broth (Sigma-Aldrich) for 3 days followed by lavage of peritoneal cavity with 10 mL cold PBS. The peritoneal cells were washed with cold PBS centrifuged at 1,000 rpm for 10 min and counted. For macrophage purification, cells were incubated at 37°C in Dulbecco's modified Eagle's medium/F12-10 medium. RNA was extracted from attached cells and used for gene expression analysis. For fluorescence-activated cell sorter (FACS) analysis, peritoneal cells were centrifuged, resuspended in Hanks' balanced salt solution, and further processed as described below.

Isolation of Adipocytes and Stromal Vascular Fraction

Adipocyte and stromal vascular fractions (SVFs) were isolated from WT and $Itch^{-/-}$ white adipose tissue (WAT) after 12 weeks of HFD as previously described (16). RNA was isolated from adipocytes and SVF and analyzed by real-time PCR. The profile of adiponectin mRNA expression was used to test the purity of the isolated fractions.

Gene Expression Analysis

Total RNA was isolated from adipose tissues, liver, peritoneal macrophages, bone marrow–derived macrophages, RAW 264.7 cells, and 3T3 F44 cells using Trizol reagents (Invitrogen Corp., Eugene, OR). Total RNA (2 μg) was reverse transcribed into cDNA using the High Capacity cDNA Archive kit (Applied Biosystems, Foster City, CA). Quantitative real-time PCR was performed, and the results were analyzed as previously described (16).

Western Blots

Western blots were performed as previously described (18). The following antibodies were used: phospho-Insr Tyr^{972}, total Insr, phospho-Ser^{473} Akt, total Akt (Cell Signaling Technology), human ITCH/AIP4 (Abcam), and mouse ITCH (BD Pharmigen).

Histological Analysis

Epididymal WAT, interscapular brown adipose tissue (BAT), liver, and intestinal tissues were obtained from mice fed an HFD for 12 weeks; specimens were fixed in 10% paraformaldehyde and embedded in paraffin. Ten-micrometer consecutive sections were then mounted on slides and stained with hematoxylin-eosin (H-E). Oil Red O staining were performed on liver sections from cryopreserved biopsies. Photomicrographs were captured with Eclipse TE 2000-S (Nikon) microscope at ×10 and ×20 magnifications. Adipose cell size was measured under the same microscope at ×10 magnification with a scale of 5 μm per unit of graduation. The diameter of 50 cells in two random microscopic fields was determined using Lucia G, version 4.61 (Build 64), software for each mouse. Severity of nonalcoholic fatty liver disease was based on the amount and types of fat (macrovesicular and microvesicular), extent of inflammation, presence of

cell degeneration (acidophil bodies, ballooning, and Mallory's hyaline), or necrosis and degree of fibrosis.

Flow Cytometry Analysis

Liver FACS analysis was performed as previously described (19). In brief, livers were digested with Collagenase 4 (Sigma-Aldrich). Samples were then subjected to FICOLL density gradient (LSM-1077; Sigma-Aldrich) and stained with CD45-APC (BD Pharmigen), CD11b-FITC (Miltenyi Biotec), and F4/80-PE (Miltenyi Biotec). Cells collected from the peritoneal cavity were stained for surface antigens CD11b-FITC (Miltenyi Biotec) and F4/80-PE (Miltenyi Biotec). Samples were analyzed using a FACScalibur (BD bioscience) running BD Cellquest Pro and analyzed with Flow JO (TreeStar, Ashland OR). Macrophages were defined as $CD45^+CD11b^+F4/80^+$.

Cholesterol and Triglycerides Assay

Cholesterol and triglycerides were extracted from liver tissues and analyzed using the Total Cholesterol Assay kit and Triglyceride Quantification kit (Cell Biolabs) according to the manufacturer's instructions.

Human Adipose Tissue Gene Expression Studies

Fifty visceral adipose tissue samples from a group of Caucasian subjects with BMI between 20 and 58 kg/m^2 recruited at the Endocrinology Service of Hospital Universitari Dr. Josep Trueta (Girona, Spain) were studied. All subjects reviewed that their body weight had been stable for at least 3 months. They had no systemic disease other than obesity, and all were free of any infections in the previous month before the study. Liver disease and thyroid dysfunction were specifically excluded by biochemical work-up. All subjects gave written informed consent after the purpose, nature, and potential risks for the study were explained to them. The Hospital Ethics Committee approved the protocol. Adipose tissue samples were obtained during elective surgical procedures (cholecystectomy, surgery of abdominal hernia, and gastric bypass surgery), washed, fragmented, and immediately flash frozen in liquid nitrogen before being stored at −80°C and used for analysis.

Immunohistochemistry

Five-micrometer sections of formalin-fixed paraffin-embedded adipose tissue were deparaffinized and rehydrated prior to antigen unmasking. Sections were incubated with anti- ITCH/AIP4 (Abcam), anti-CD68 (Santa Cruz Biotechnology), and anti-CD3 (Thermo Scientific, Fremont, CA). Sections were counterstained with hematoxylin and examined under a Nikon Eclipse 90i microscope. As a negative control, the procedure was performed in the absence of primary antibody.

Statistical Analyses

Results of the experimental studies are means ± SD. Statistical analyses were performed using one-way ANOVA or the unpaired Student t test as indicated. Linear correlation analysis was performed using the Spearman test. Values of $P < 0.05$ were considered statistically significant.

RESULTS

Metabolic and Immunologic Phenotype of Itch$^{−/−}$ Mice

At 6 weeks of age, Itch$^{−/−}$ mice fed standard chow showed lower weight and lower fasting blood glucose levels compared with the same age WT littermates (Fig. 1A and B). These differences tended to disappear with aging in mice fed a standard chow. Itch$^{−/−}$ mice show a Th2 polarization of lymphocytes due to the high expression of IL-4 and IL-13 (12). To determine whether an increase in Th2 lymphocytes results in an increase in M2 macrophage polarization, we evaluated gene expression of M1 and M2 markers of peritoneal macrophages from WT and Itch$^{−/−}$ mice fed standard chow after thioglycollate broth stimulation. Peritoneal exudates from WT and Itch$^{−/−}$ mice revealed similar levels of isolated $CD11b^+F4/80^+$ cells (Supplementary Fig. 1A). However, Itch$^{−/−}$ macrophages showed a significant increase in the expression of M2 markers Mgl2, Arg1, and Ym1. The expression of M1 markers remained similar (Fig. 1C). In vitro downregulation of itch expression with small interfering RNA in bone marrow–derived macrophages and in RAW 267.4 cells, a mouse macrophage cell line, resulted in a reduction of IL-1β and EMR1 and an increase in IL-10 expression after treatment with a combination of LPS and IFN-γ, while after IL-4 stimulation we found only a reduction of EMR1 (Supplementary Fig. 1B and C).

Metabolic Effect of Diet-Induced Obesity on Itch$^{−/−}$ Mice

Western blot analysis revealed that ITCH is expressed in both adipocyte fraction (AF) and SVFs in mice (Supplementary Fig. 1D). For evaluation of the effect of ITCH deficiency in the development of obesity, Itch$^{−/−}$ and WT mice were fed an HFD or standard chow for 12 weeks. After 12 weeks, mice fed standard chow did not show differences in body weight, blood glucose, or serum insulin levels. During the HFD treatment, Itch$^{−/−}$ mice did not show any increase in body weight, and body weight curve was at all times significantly lower in Itch$^{−/−}$ mice compared with WT (Fig. 2A and B). After 12 weeks of HFD, Itch$^{−/−}$ mice showed significantly lower blood glucose levels in the fasting state (Fig. 2C) and improved glucose tolerance as demonstrated by the results obtained from blood glucose and insulin measurement during intraperitoneal glucose tolerance test analysis (Fig. 2D and E). Itch$^{−/−}$ mice showed decreased serum insulin levels both in the fasting and in the random fed state and presented significantly lower values of homeostasis model assessment of insulin resistance index (Fig. 2F and G). In muscle from Itch$^{−/−}$ mice compared with WT, we found a significant increased phosphorylation of Tyr^{972} insulin receptor (Insr) and of Ser^{473} AKT after 6 h of refeeding (Fig. 2H). Itch$^{+/−}$ mice
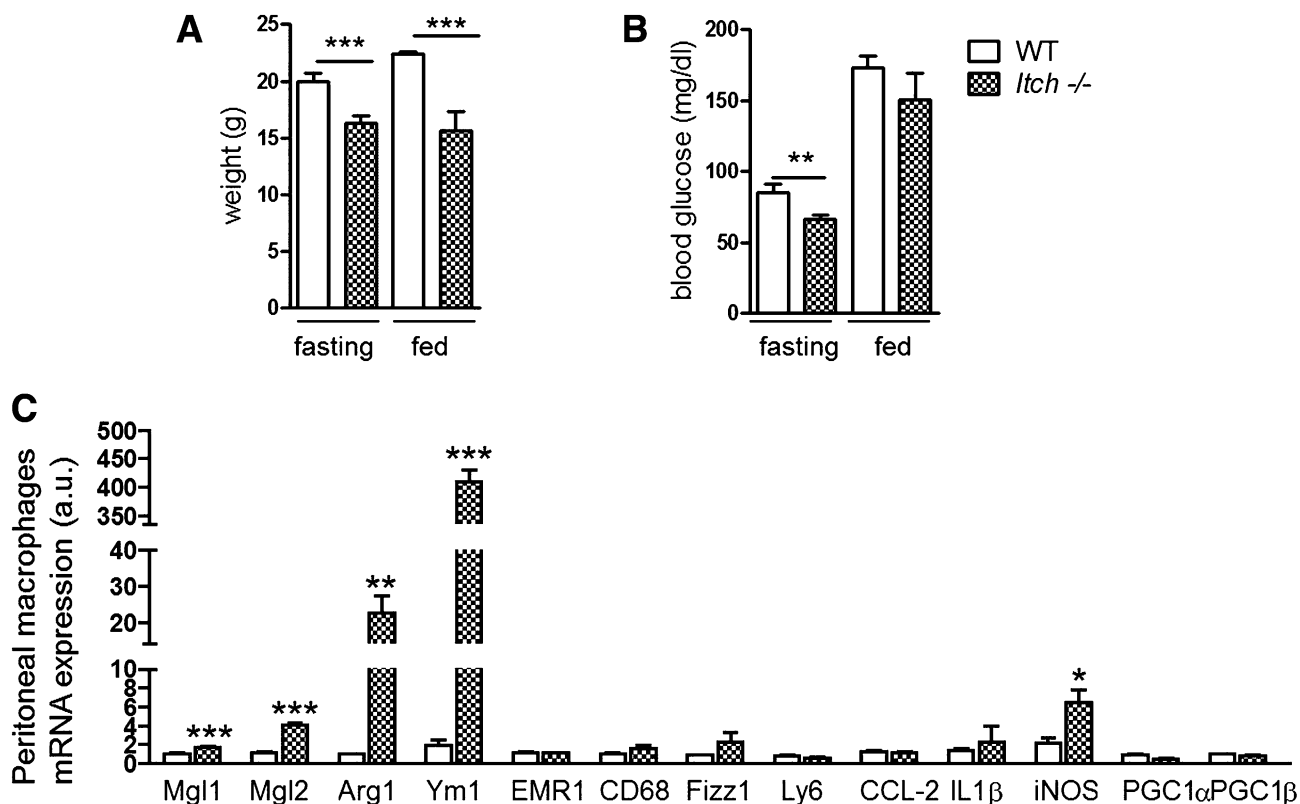
Figure 1—Metabolic characterization of Itch$^{-/-}$ mice. Six-week-old WT and Itch$^{-/-}$ mice fed a ND. Weight (A) and blood glucose concentration (B) (n = 8 per group; **P < 0.005, ***P < 0.001, Student t test). Data are means ± SD. C: Peritoneal macrophage gene expression analysis. Expression of mRNA was determined by real-time PCR and normalized to β-actin (n = 4 per group; *P < 0.05, **P < 0.005, ***P < 0.001, Student t test). Data are means ± SD. iNOS, inducible nitric oxide synthase; a.u., arbitrary units.

were only partially protected during HFD, since at 12 weeks of HFD they were comparable with WT (Supplementary Fig. 2). Indirect calorimetric measurement showed that Itch$^{-/-}$ mice exhibited a significant increase in VO$_2$ and VCO$_2$ and a mild significant decrease in respiratory exchange ratio (RER) (VCO$_2$/VO$_2$) (Fig. 3A–C), while locomotor activity and food intake remained similar in the two groups (Fig. 3D and E). Consistent with a leaner phenotype, Itch$^{-/-}$ mice fed an HFD have reduced blood pressure and an increased heart frequency compared with WT littermates (Fig. 3F and G). Itch$^{-/-}$ mice fed an HFD also showed significantly reduced levels of total cholesterol (Fig. 3H) and mild but not significant reduced levels of hepatic transaminases (ALT and AST) compared with WT (Fig. 3M and N). When HFD is interrupted, Itch$^{-/-}$ mice showed the same trend of body weight observed in WT mice fed a ND during physiological aging (Supplementary Fig. 3 and Fig. 2A).

Effect of ITCH Deficiency on WAT During HFD

For evaluation of the effect of ITCH deficiency on adipose tissue in a context of diet-induced obesity, epididymal fat pads from Itch$^{-/-}$ and WT mice were analyzed. After 12 weeks of HFD, Itch$^{-/-}$ mice showed reduced fat pad mass compared with WT littermates (Supplementary Fig. 3B and C); reduction in body weight and fat pad mass

were not associated with malabsorption or intestinal inflammation as showed in intestinal permeability assay and intestinal histological examination (Supplementary Fig. 3D and E). In vitro studies performed on preadipocytes, 3T3F44 cells, transfected with itch small interfering RNA and then differentiated into adipocytes, suggested that ITCH downregulation is not related to reduced adipocyte differentiation (Supplementary Fig. 3F). Histological examination of adipose tissue sections from HFD mice showed reduced adipocyte size and higher density of smaller adipocytes in Itch$^{-/-}$ compared with WT (Fig. 4A). Next, to explore the mechanisms underlying the effect of ITCH deficiency on adipose tissue function we analyzed the expression of genes involved in inflammation, glucose/lipid metabolism, and mitochondrial function. To test whether the effect of ITCH was dependent on nutritional state, we analyzed mice both in the fasting and in the refed state. In Itch$^{-/-}$ WAT, we observed significantly increased levels of M2 markers such as Mgl2, Ym1, and IL-4 in both nutritional states, while IL-13 and Agr1 mRNA levels were significantly upregulated only in the fasting state; we also observed a significantly lower expression of EMR1 and TNF-α in the fasting state (Fig. 4B). Analysis of genes involved in glucose and lipid metabolism showed significantly increased levels of PPAR-α and SREBP1 in both
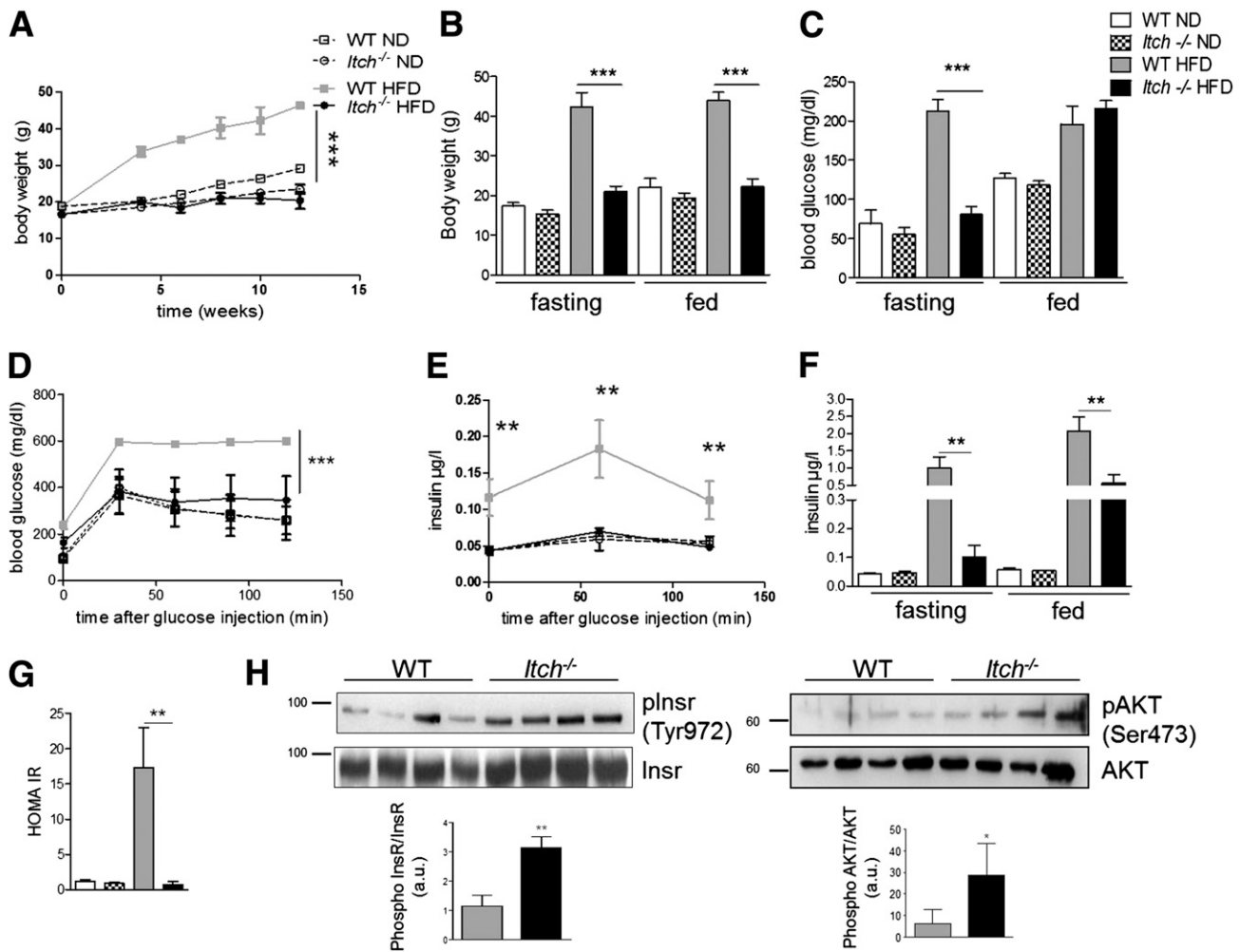
Figure 2—$Itch^{-/-}$ mice are protected against HFD-induced obesity and insulin resistance. WT and $Itch^{-/-}$ mice were fed a ND or HFD for 12 weeks. A: Body weight curve during the treatment ($n = 8$ per group; ***$P < 0.001$, one-way ANOVA). Data are means ± SD. Body weight (B) and blood glucose levels (C) after 12 weeks of HFD in the fasting and fed state ($n = 8$ per group, ***$P < 0.001$; Student t test). Data are means ± SD. Blood glucose levels (D) and serum insulin levels (E) during intraperitoneal glucose tolerance test at 12 weeks of HFD ($n = 8$ per group; **$P < 0.005$, ***$P < 0.001$, one-way ANOVA). Data are means ± SD. F: Serum insulin levels at 12 weeks of HFD in the fasting and fed state. **$P < 0.01$. G: Homeostasis assessment of insulin resistance (HOMA IR) ($n = 8$ per group; **$P < 0.005$, Student t test). Data are means ± SD. H: Muscle Tyr^{972} Insr and Ser^{473} AKT phosphorylation ($n = 4$ per group; *$P < 0.05$, **$P < 0.005$, Student t test). Data are means ± SD. a.u., arbitrary units; pInsr, phospho-Insr.

nutritional states; PPAR-γ was shown to be significantly upregulated only in the refed state, while we found a significant increase in PPAR-δ in the fasting condition. We found a slight but not significant increase in C/EBP-α in both nutritional conditions and a significant increase in C/EBP-β expression in the fasting state (Fig. 4B). Genes involved in mitochondrial function, such as PCG1-α, PGC1-β, Tfam, NRF1, ACOX1, SIRT1, eNOS, and UCP3, were significantly upregulated in $Itch^{-/-}$ adipose tissue compared with WT in both nutritional states (Fig. 4B). Gene expression analysis in isolated adipocyte and SVF from WAT of WT and $Itch^{-/-}$ mice fed an HFD showed an important contribution of SVF in modulating genes involved in mitochondrial function and energy expenditure. Indeed, PGC1-α, PGC1-β, ACOX1, NRF1, Tfam, SIRT1, and UCP3 were increased in SVF of $Itch^{-/-}$

mice compared with WT (Fig. 5). Furthermore, the expression of UCP1 was significantly increased in the SVF of $Itch^{-/-}$ mice, suggesting an important role of the SVF in the metabolic phenotype of $Itch^{-/-}$ mice. The SVF from $Itch^{-/-}$ mice showed a significant upregulation of PPAR-γ gene expression (Fig. 5), whose importance in M2 polarization and oxidative capacity of tissue macrophages has been demonstrated (20,21). To further investigate whether the overall improvement of metabolic condition observed in HFD $Itch^{-/-}$ mice depended on specific contribution of immune cells, we performed bone marrow transplantation experiments, obtaining chimeras mice. Our preliminary data showed that transplantation of bone marrow cells from $Itch^{-/-}$ mice to WT littermates conferred protection from glucose intolerance after 6 weeks of HFD (Supplementary Fig. 4A and B)
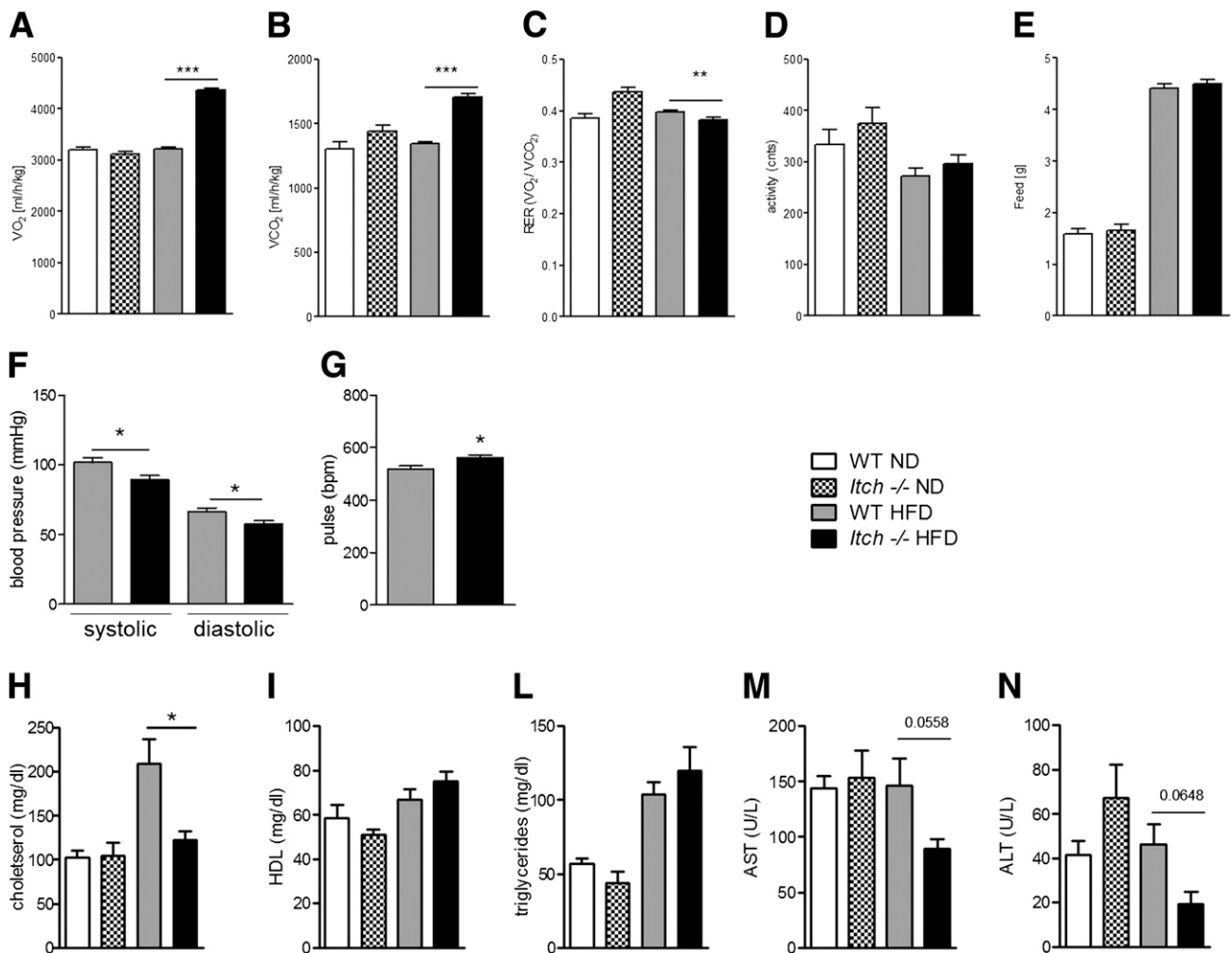
Figure 3—$Itch^{-/-}$ mice fed an HFD show accelerated metabolism compared with WT. WT and $Itch^{-/-}$ mice were fed an HFD for 12 weeks. Mean 24 h for VO_2 values (A), CO_2 production (VCO_2) (B), RER (C), locomotor activity (D), and food intake (E). Systolic and diastolic blood pressure (F). Pulse per minute (G). Fasting serum concentration of total cholesterol (H), HDL (I), triglycerides (L), AST (M), and ALT (N) (n = 6 per group; *P < 0.05, **P < 0.005, ***P < 0.001, Student t test). Data are means ± SD. Cnts, counts/h.

Effect of ITCH Deficiency on BAT and Liver During HFD

Given the results obtained from WAT, we investigated the condition of BAT from WT and $Itch^{-/-}$ mice fed an HFD. Histological examination of BAT sections, stained with H-E, showed reduced adipocytes size and higher density of smaller adipocytes in $Itch^{-/-}$ mice compared with WT littermates fed an HFD (Fig. 6A). Gene expression analysis of BAT showed a significantly higher expression of M2 markers such as Arg1, YM1, IL-4, and IL-13 and a lower expression of EMR1 in $Itch^{-/-}$ tissue compared with WT (Fig. 6B). mRNA expression of UCP3 resulted increased in $Itch^{-/-}$ mice (Fig. 6B). Given that hepatic steatosis is one of the most common consequences of nutrient overload in mouse models, we performed histological and molecular analysis on livers from WT and $Itch^{-/-}$ mice fed an HFD. Histological analysis showed that $Itch^{-/-}$ mice were protected from the onset of macrovesicular steatosis as observed in WT littermates; Oil Red O staining confirmed a reduction in

lipid accumulation in liver from $Itch^{-/-}$ mice (Fig. 6C). Triglycerides, but not cholesterol levels, were significantly lower in $Itch^{-/-}$ livers compared with WT (Fig. 6D). FACS analysis revealed that inflammatory $CD45^+CD11b^+F4/80^+$ cells were reduced (Fig. 6E), while gene expression of IL-13, UCP2, and transforming growth factor-β was upregulated in $Itch^{-/-}$ liver compared with WT (Fig. 6F).

Itch Gene Expression Correlates With M2 Markers CD206 in Human Adipose Tissue of Obese Patients

To exploit the significance of ITCH effects on human adipose tissue inflammation, we analyzed its expression in human adipose tissue biopsies. ITCH protein expression was observed both in SVF and adipocyte fractions in human subjects (Fig. 7A). Immunohistochemical analysis confirmed that ITCH is expressed in $CD68^+$ and $CD3^+$ cells (Fig. 7B). Analysis of itch expression in subjects with different degrees of BMI and insulin sensitivity
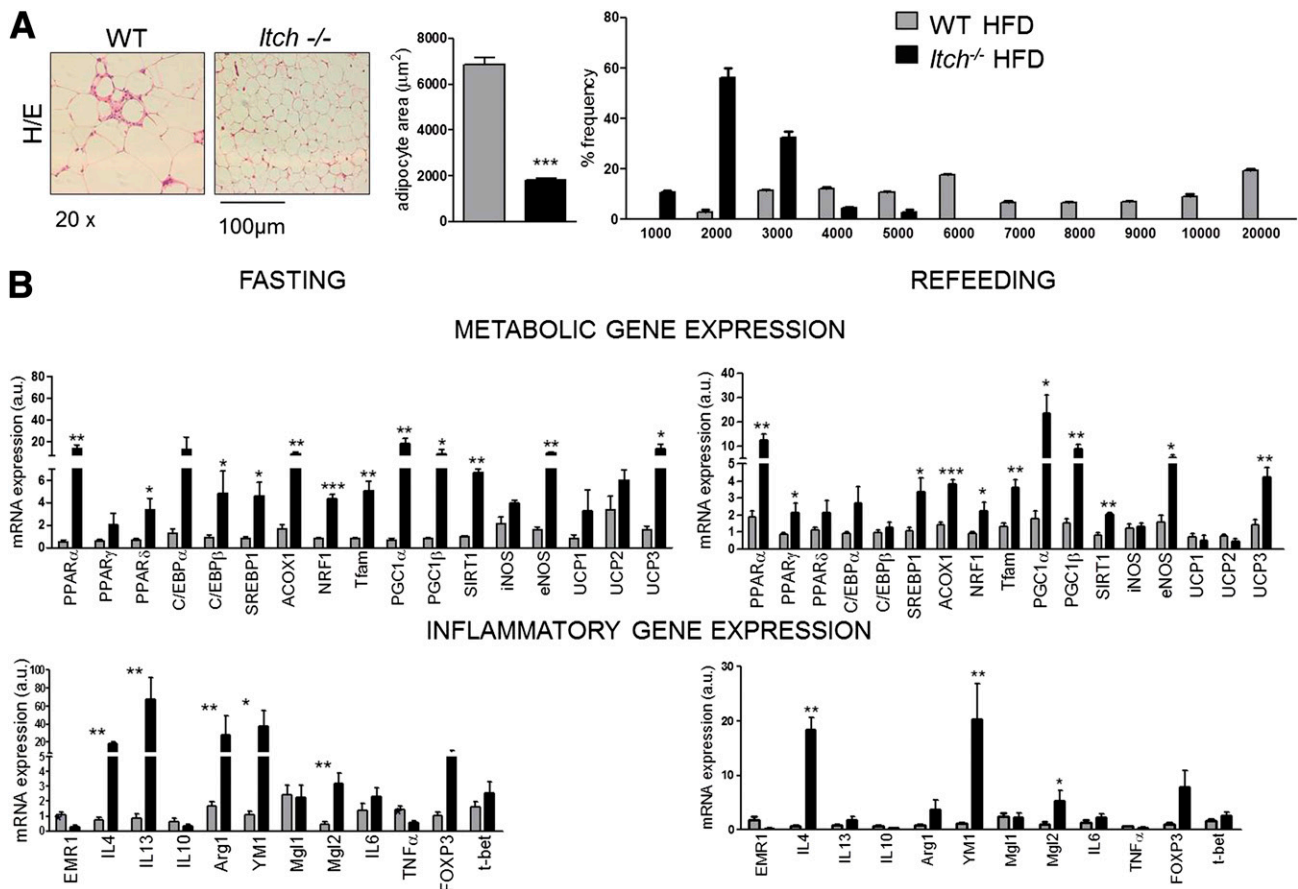
Figure 4—Effect of ITCH deficiency on WAT during HFD. Epididymal adipose tissues from WT and *Itch*$^{-/-}$ mice after 12 weeks of HFD were harvested and analyzed. *A*: Representative sections of adipose tissue stained with H-E, mean adipocyte area, and frequency distribution of adipocyte area. *B*: Metabolic and inflammatory gene expression. Expression of mRNA was determined by real-time PCR and normalized to β-actin (*n* = 5 per group; *$P < 0.05$, **$P < 0.005$, ***$P < 0.001$, Student *t* test). Data are means ± SD. a.u., arbitrary units.

(Supplementary Table 1) revealed a significant negative correlation between *Itch* and the expression of CD206, a marker of M2 macrophages (Fig. 7*C*); moreover, the CD206-to-CD68 ratio was also found to be significantly negatively correlated to *itch* expression (Fig. 7*D*), indicating that there is a link between *itch* expression and the inflammatory cell phenotype in adipose tissue. In a multiple linear regression analysis, *itch* contributed to CD206/CD68 variance after BMI, age, and total cholesterol levels were controlled for (*P* = 0.030) (Supplementary Table 1 and data not shown).

DISCUSSION

Growing evidence suggests a predominant role of ATMs in establishing and maintaining the inflammatory status of adipose tissue in obesity (22,23). Adipose tissue from lean subjects is predominantly characterized by the presence of CD4$^+$ CD25$^+$ Treg cells and M2 macrophages (22). Macrophage differentiation into either M1 or M2 occurs in response to Th1 or Th2 cytokine (IFN-γ/TNF-α or IL-4/IL-13), respectfully, thus stimulating a proinflammatory (M1) or reparative (M2) response (24). M2

macrophages can promote oxidative metabolism and augment the energy expenditure of infiltrating tissues. Many recent studies support their potential role in protection from obesity and insulin resistance through the expression of PPAR-γ and PGC-1β (20–22). Overall, these findings suggest that strategies pointed to increased M2-to-M1 ratio in adipose tissue could help to dampen the onset of insulin resistance, although direct demonstrations are still missing. ITCH E3 ubiquitin ligase has been shown to control several inflammatory pathways both in immune and in nonimmune cells. In particular, ITCH is required for JunB proteasomal degradation in lymphocytes, and its deficiency in vivo causes aberrant IL-4 production and Th2 polarization (12). Therefore, we tested whether a limit to ITCH expression in vivo, using the *Itch*$^{-/-}$ mouse, could result in an increased Th2/M2 polarization leading to potential beneficial metabolic effects in the context of diet-induced obesity. Our results showed that ITCH deficiency were associated with lower weight and blood glucose levels in young mice compared with WT littermates, but these differences disappeared when the animals reached adult
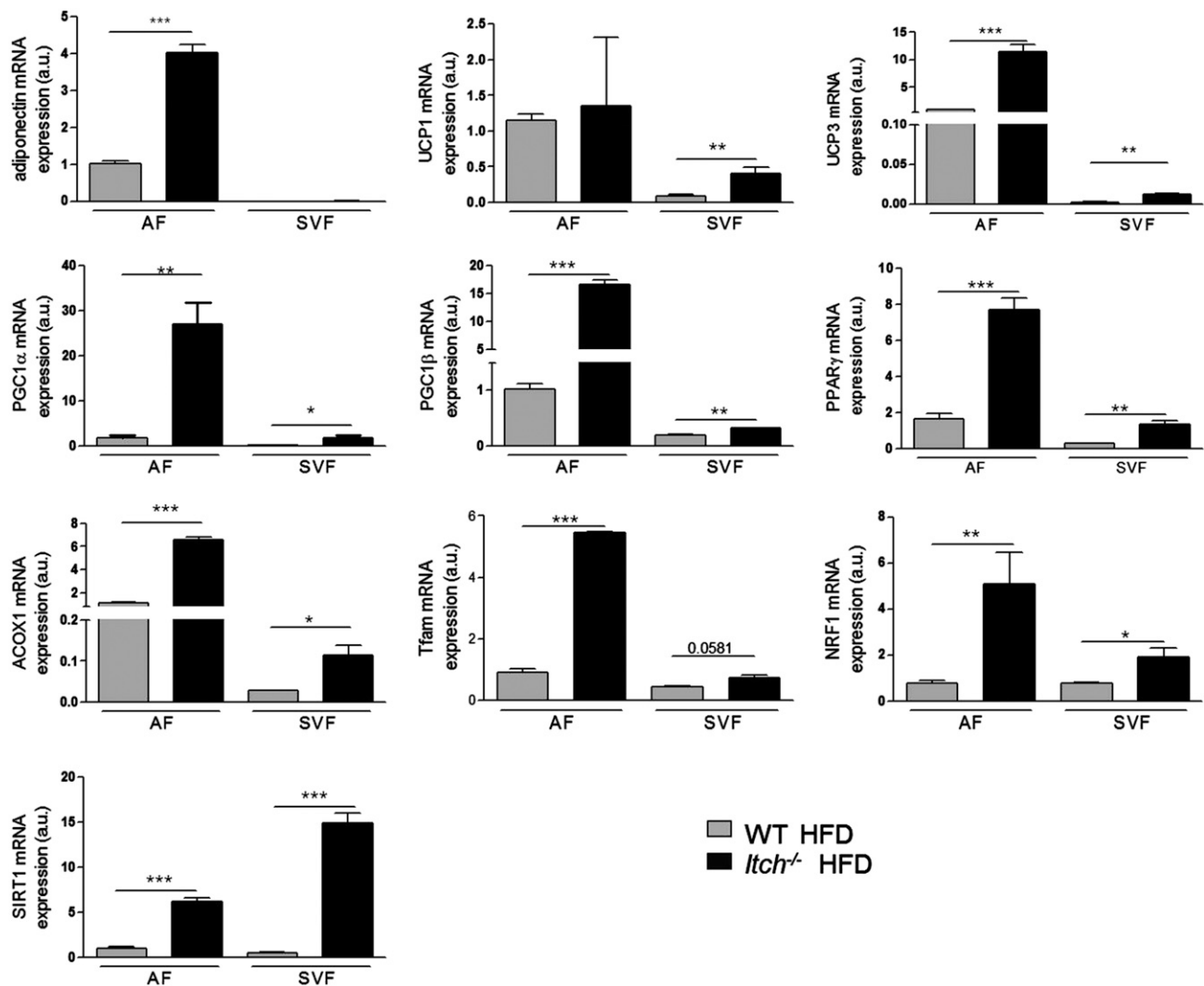
Figure 5—Effect of ITCH deficiency on gene expression of SVF and adipocyte fraction (AF) from WAT. Gene expression analysis of SVF and AF from WT and *Itch*$^{-/-}$ mice fed an HFD for 12 weeks (*n* = 5 per group; *P < 0.05, **P < 0.005, ***P < 0.001, Student *t* test). Data are means ± SD. Expression of mRNA was determined by real-time PCR and normalized to β-actin. a.u., arbitrary units.

age on a standard diet regimen. Conversely, a lipid nutrient overload induced through HFD had a dramatic effect on both weight and consequent glucose tolerance in *Itch*$^{-/-}$ mice. These effects were associated with accelerated metabolism measured by VO$_2$ consumption, VCO$_2$ production, and their ratio (RER) and with maintenance of high expression of M2 macrophage markers and low expression of M1 macrophage markers in both BAT and WAT. Our results suggest that a strategy to implement M2 macrophage function in obesity could promote either weight loss or the improvement of insulin resistance in both fasting and the refed state, suggesting an effect on the dynamic regulation of inflammation during the refeeding process. Whether such a strategy may be translated to human obesity, with the use of appropriate diet regimens, is at this stage unknown. BAT from *Itch*$^{-/-}$ mice fed an HFD presented smaller

adipocytes with high density compared with WT tissue and expressed an anti-inflammatory pattern similar to what we found in WAT. The comparable effect of ITCH deficiency in WAT and BAT might suggest that a balance between M2 and M1 could affect both storage/endocrine functions typical of WAT as well as energetic functions of BAT. Loss of ITCH was also associated with increased UCP3 expression both in WAT and in BAT, and we can speculate that this may be related to the highest presence of M2 macrophages that are known to produce low levels of catecholamines within the adipose tissue itself (25). Although we cannot exclude that ITCH deficiency could promote the transdifferentiation of BAT into WAT, we found no differences in an established marker of brown adipocytes such as PRDM16 (at protein levels, data not shown) in WAT. UCP1 and PPAR-γ expression were significantly increased in SVF isolated from WAT of
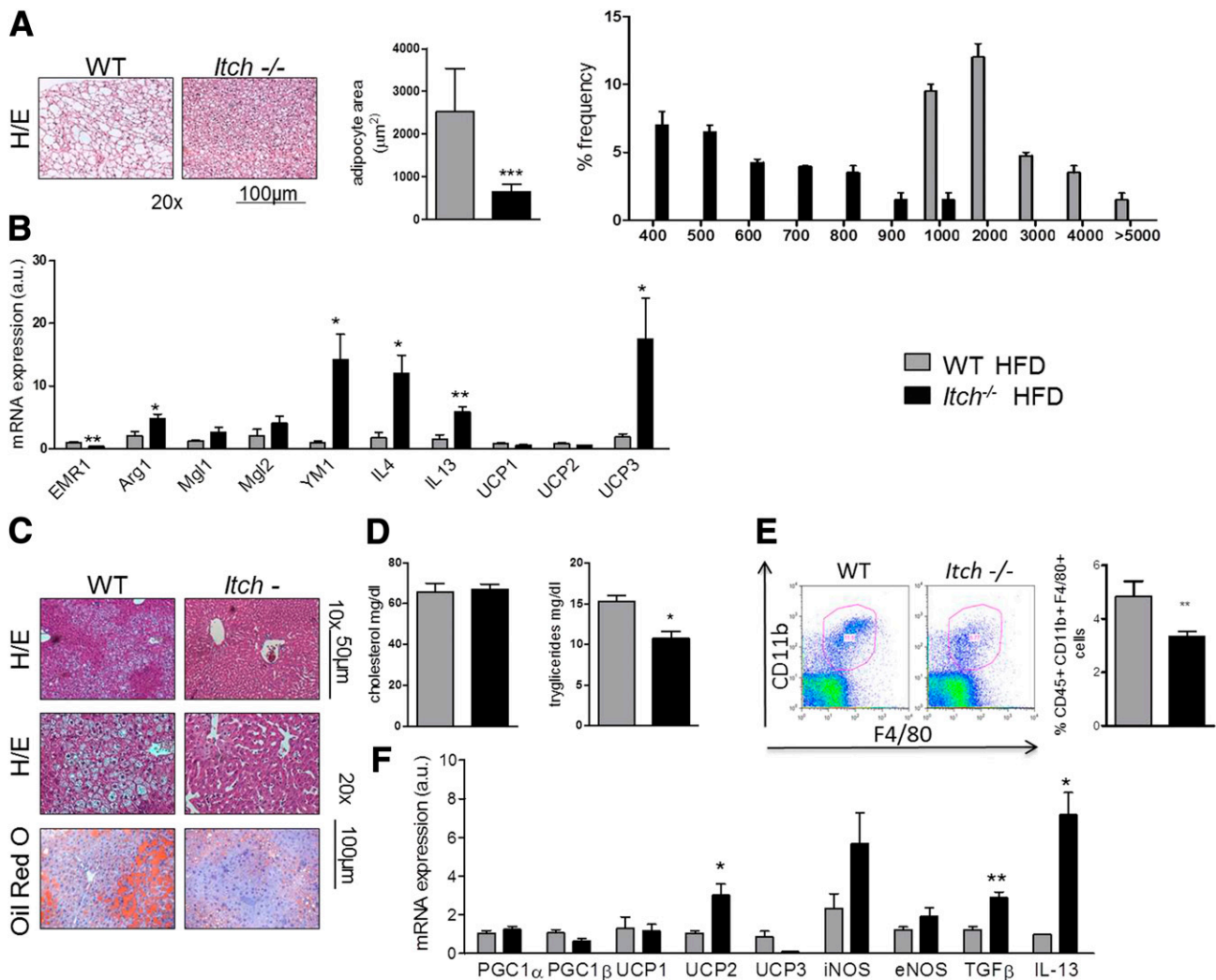
Figure 6—Effect of ITCH deficiency on BAT and liver during HFD. Representative sections of BAT stained with *H–E*, mean adipocyte area, and frequency distribution of adipocyte area (*A*). BAT gene expression analysis (*B*). Representative sections of livers stained with *H–E* and Oil Red O (310 and 320, respectively) (*C*). Liver cholesterol and triglycerides levels (*D*). *E*: FACS analysis of liver CD45+CD11b+F4/80+ cells. *Left*: Representative dot plots. *Right*: Summary data. Numbers on dot plots indicate the percentage of cells in that gate for that particular experiment. *F*: Liver gene expression analysis. Expression of mRNA was determined by real-time PCR and normalized to β-actin ($n = 5$ per group). *$P < 0.05$; **$P < 0.001$; ***$P < 0.001$, Student t test. Data are means ± SD. a.u., arbitrary units.

$Itch^{-/-}$ mice, suggesting potential energetic effects of SVF cells such as polarized M2 macrophages. These findings have been corroborated by our preliminary results of bone marrow transplantation experiments. In livers from $Itch^{-/-}$ mice, we found high levels of IL-13, which could contribute to explain the glucose control in $Itch^{-/-}$ mice; indeed, recently, a role for IL-13 in controlling glucose tolerance was proposed. IL-13 suppresses hepatic glucose production through signal transducer and activator of transcription 3 (STAT3) activation, and then the IL-13 deficiency leads to hyperglycemia and insulin resistance (26). Next, in order to evaluate whether the effect of ITCH deficiency in mice may be translated in human specimens we analyzed human biopsies of adipose tissue.

The cross-sectional analysis of adipose biopsies clearly linked *itch* levels to adipose tissue inflammation, particularly with the M2-to-M1 ratio expressed using two well-accepted markers for these macrophage polarization states.

We found that when the HFD was interrupted, $Itch^{-/-}$ mice tended to maintain their weight. These data suggest that the effect of *itch* deficiency on obesity is mediated by diet-induced inflammation, and apparently in the absence of inflammatory stimulus (HFD) *itch* deficiency does not affect metabolic phenotype of mice. Translating our results to a therapeutic perspective, we find it tempting to speculate on the Th2 response as a treatment for obesity and its metabolic sequels under certain conditions (27). The appropriate dietary regimen
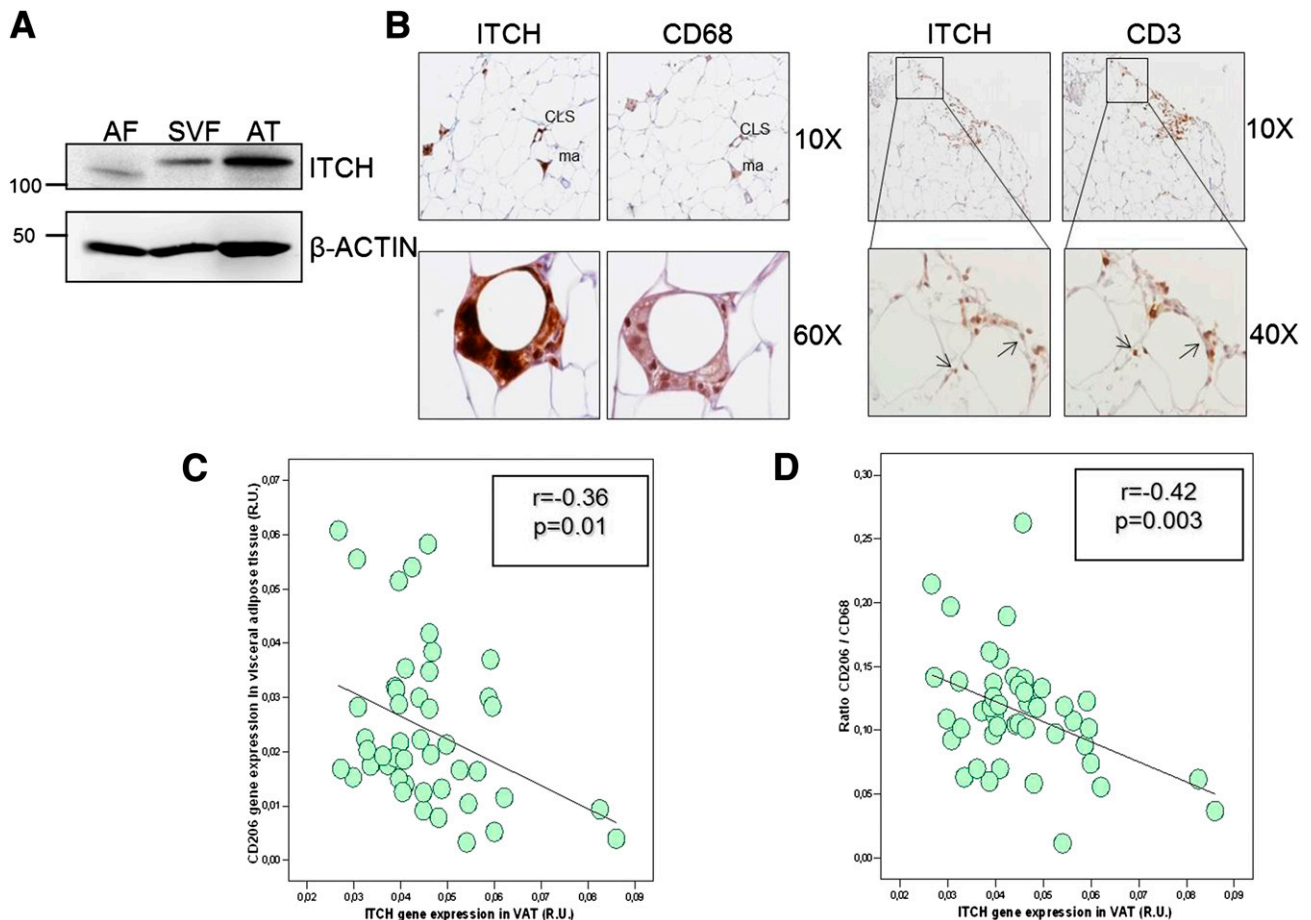
Figure 7—Representative Western blot analysis of ITCH protein in adipose tissue (AT), isolated adipocytes (adipocyte fraction [AF]), and SVFs (*A*). Representative Western blot analysis of ITCH protein in AT, isolated adipocytes (AF), and SVFs (*B*). Images are representative of adipose tissue sections collected from five subjects. CLS, crown-like structure; ma, macrophage. The arrows indicate ITCH- and CD3-positive cells. Correlation between *Itch* and CD-206 mRNA (*C*) expression ($r = -0.36$, $P = 0.01$) and CD206-to-CD68 ratio (*D*) ($r = -0.42$, $P = 0.003$) in human adipose tissue ($n = 50$). Expression of mRNA was determined by real-time PCR and normalized to cyclophilin A. R.U., relative units; VAT, visceral adipose tissue.

to be administered during an anti-inflammatory metabolic treatment is also a relevant issue, since some forms of lipids are known to positively or negatively affect the inflammatory response (28,29). The effect of the inhibition of ITCH on adipose tissue might be additive to other pathways that have been demonstrated to be relevant to dampen metabolic inflammation in skeletal muscle, such as the TNF-α–converting enzyme pathway, which is positively restrained by pioglitazone, a PPAR-γ agonist with anti-inflammatory effects, in patients with type 2 diabetes (30,31).

Since *itch* knockdown did not interfere with adipogenesis and only mildly interfered with M1 polarization in vitro and $Itch^{-/-}$ mice revealed normal food intake and no intestinal inflammation, it is tempting to speculate that the protective effect observed in vivo is dependent on macrophage infiltration that occurs in adipose tissue during the progression of obesity. Nevertheless, our data suggest that ITCH acts as a factor to

restrain Th2 bias in vivo and its consequences on obesity and metabolic inflammation, especially when a diet rich in lipids is imposed. Two possible ITCH targets to be explored in more mechanistic models are p73 and promyelocytic leukemia (PML). ITCH is known to negatively affect p73 (32,33), which regulates PML protein levels (34). PML deficiency was associated with diet-induced obesity (35,36), and p73-null macrophages were biased to M1 polarization in vivo (37); we preliminarily observed that PML is increased in both WAT and BAT in $Itch^{-/-}$ mice (Supplementary Fig. 5), which supports a role for PML in metabolic disorders, although further studies are necessary to understand whether the ITCH/p73/PML pathway acts at the monocyte/macrophage or adipocyte level.

Our results confirm the evidence that macrophage-mediated inflammation in adipose tissue plays an important role in the development of obesity and its metabolic complications. The Th2/M2 bias in $Itch^{-/-}$ mice

causes chronic M2 polarization of macrophages in-filtrating adipose tissue protecting from weight gain and consequent metabolic disturbances during an obesogenic stimulus. Taken together, our data pinpoint a role for ITCH-mediated pathways in the regulation of the complex interactions between innate immunity and metabolism.

References

1. Weisberg SP, McCann D, Desai M, Rosenbaum M, Leibel RL, Ferrante AW Jr. Obesity is associated with macrophage accumulation in adipose tissue. J Clin Invest 2003;112:1796–1808

2. Stefan N, Häring HU. The metabolically benign and malignant fatty liver. Diabetes 2011;60:2011–2017

3. Fernández-Real JM, Pickup JC. Innate immunity, insulin resistance and type 2 diabetes. Diabetologia 2012;55:273–278

4. Gregor MF, Hotamisligil GS. Inflammatory mechanisms in obesity. Annu Rev Immunol 2011;29:415–445

5. Osborn O, Olefsky JM. The cellular and signaling networks linking the immune system and metabolism in disease. Nat Med 2012;18:363–374

6. Biswas SK, Mantovani A. Orchestration of metabolism by macrophages. Cell Metab 2012;15:432–437

7. Sica A, Mantovani A. Macrophage plasticity and polarization: in vivo veritas. J Clin Invest 2012;122:787–795

8. Harford KA, Reynolds CM, McGillicuddy FC, Roche HM. Fats, inflammation and insulin resistance: insights to the role of macrophage and T-cell accumulation in adipose tissue. Proc Nutr Soc 2011;70:408–417

9. Lacy-Hulbert A, Moore KJ. Designer macrophages: oxidative metabolism fuels inflammation repair. Cell Metab 2006;4:7–8

10. Perry WL, Hustad CM, Swing DA, O'Sullivan TN, Jenkins NA, Copeland NG. The itchy locus encodes a novel ubiquitin protein ligase that is disrupted in a18H mice. Nat Genet 1998;18:143–146

11. Melino G, Gallagher E, Aqeilan RI, et al. Itch: a HECT-type E3 ligase regulating immunity, skin and cancer. Cell Death Differ 2008;15:1103–1112

12. Fang D, Elly C, Gao B, et al. Dysregulation of T lymphocyte function in itchy mice: a role for Itch in TH2 differentiation. Nat Immunol 2002;3:281–287

13. Parravicini V, Field AC, Tomlinson PD, Basson MA, Zamoyska R. Itch-/-alphabeta and gammadelta T cells independently contribute to autoimmunity in Itchy mice. Blood 2008;111:4273–7282

14. Casagrande V, Menghini R, Menini S, et al. Overexpression of tissue inhibitor of metalloproteinase 3 in macrophages reduces atherosclerosis in low-density lipoprotein receptor knockout mice. Arterioscler Thromb Vasc Biol 2012;32:74–81

15. Menghini R, Menini S, Amoruso R, et al. Tissue inhibitor of metalloproteinase 3 deficiency causes hepatic steatosis and adipose tissue inflammation in mice. Gastroenterology 2009;136:663–672, e4

16. Menghini R, Casagrande V, Menini S, et al. TIMP3 overexpression in macrophages protects from insulin resistance, adipose inflammation, and nonalcoholic fatty liver disease in mice. Diabetes 2012;61:454–462

17. Zhang X, Goncalves R, Mosser DM. The isolation and characterization of murine macrophages. Curr Protoc Immunol 2008;Chapter 14:Unit 14.1

18. Menghini R, Marchetti V, Cardellini M, et al. Phosphorylation of GATA2 by Akt increases adipose tissue differentiation and reduces adipose tissue-related inflammation: a novel pathway linking obesity to atherosclerosis. Circulation 2005;111:1946–1953

19. Karlmark KR, Zimmermann HW, Roderburg C, et al. The fractalkine receptor CX3CR1 protects against liver fibrosis by controlling differentiation and survival of infiltrating hepatic monocytes. Hepathology 2010;52:1769–1782

20. Odegaard JI, Chawla A. Alternative macrophage activation and metabolism. Annu Rev Pathol 2011;6:275–297

21. Odegaard JI, Ricardo-Gonzalez RR, Goforth MH, et al. Macrophage-specific PPARgamma controls alternative activation and improves insulin resistance. Nature 2007;447:1116–1120

22. Chawla A, Nguyen KD, Goh YP. Macrophage-mediated inflammation in metabolic disease. Nat Rev Immunol 2011;11:738–749

23. Kanneganti TD, Dixit VD. Immunological complications of obesity. Nat Immunol 2012;13:707–712

24. Mantovani A, Biswas SK, Galdiero MR, Sica A, Locati M. Macrophage plasticity and polarization in tissue repair and remodelling. J Pathol 2013;229:176–185

25. Nguyen KD, Qiu Y, Cui X, et al. Alternatively activated macrophages produce catecholamines to sustain adaptive thermogenesis. Nature 2011;480:104–108

26. Stanya KJ, Jacobi D, Liu S, et al. Direct control of hepatic glucose production by interleukin-13 in mice. J Clin Invest 2013;123:261–271

27. Yang Z, Grinchuk V, Smith A, et al. Parasitic nematode-induced modulation of body weight and associated metabolic dysfunction in mouse models of obesity. Infect Immun 2013;81:1905–1914

28. MacLean E, Madsen N, Vliagoftis H, Field C, Cameron L. n-3 Fatty acids inhibit transcription of human IL-13: implications for development of T helper type 2 immune responses. Br J Nutr 2013;109:990–1000

29. Maijó M, Miró L, Polo J, et al. Dietary plasma proteins modulate the adaptive immune response in mice with acute lung inflammation. J Nutr 2012;142:264–270

30. Monroy A, Kamath S, Chavez AO, et al. Impaired regulation of the TNF-alpha converting enzyme/tissue inhibitor of metalloproteinase 3 proteolytic system in skeletal muscle of obese type 2 diabetic patients: a new mechanism of insulin resistance in humans. Diabetologia 2009;52:2169–2181

31. Tripathy D, Daniele G, Fiorentino TV, et al. Pioglitazone improves glucose metabolism and modulates skeletal muscle TIMP-3-TACE dyad in type 2

diabetes mellitus: a randomised, double-blind, placebo-controlled, mechanistic study. Diabetologia 2013;56:2153–2163

32. Oberst A, Rossi M, Salomoni P, et al. Regulation of the p73 protein stability and degradation. Biochem Biophys Res Commun 2005;331:707–712

33. Rossi M, De Laurenzi V, Munarriz E, et al. The ubiquitin-protein ligase Itch regulates p73 stability. EMBO J 2005;24:836–848

34. Lapi E, Di Agostino S, Donzelli S, et al. PML, YAP, and p73 are components of a proapoptotic autoregulatory feedback loop. Mol Cell 2008;32:803–814

35. Ito K, Carracedo A, Weiss D, et al. A PML–PPAR-δ pathway for fatty acid oxidation regulates hematopoietic stem cell maintenance. Nat Med 2012; 18:1350–1358

36. Carracedo A, Weiss D, Leliaert AK, et al. A metabolic prosurvival role for PML in breast cancer. J Clin Invest 2012;122:3088–3100

37. Tomasini R, Secq V, Pouyet L, et al. TAp73 is required for macrophage-mediated innate immunity and the resolution of inflammatory responses. Cell Death Differ 2013;20:293–301